

In the following subsections, the proposed algorithm is compared against the centralized (MPCOPF) algorithm in terms of resultant optimal control variables, optimality gap in objective function and computational performance. Secondly, the resultant control variables are tested for ACOPF feasibility against OpenDSS. Section -A describes the comparison over a 5 time-period horizon with an additional focus on describing the workflow of the MPDOPF algorithm. Section -B describes the comparison over a 10 time-period horizon to test for the scalability of the MPDOPF algorithm.

A. Simulation Results

Table I represents a comparison between MPCOPF and MPDOPF in their problem scope, results and computational performance.

1) Biggest Subproblem vs Computational Performance:

This first section of the table, 'Biggest subproblem' provides specifics of the 'computational bottleneck' encountered by either algorithm during its course. As described in ??, the bottleneck represents the OPF subproblem which is computationally the most intensive, and thus is a key indicator of the expected time the algorithm will take to complete. As can be seen in the third section 'Computation', there is more than a 10x speedup in computation time with MPDOPF, despite the fact that 5 such iterations were performed, totalling to 20 OPF calls over the 4 areas of the Test System.

2) Optimality of Objective Function and Control Values:

The second section of the table 'Simulation results' showcases that MPDOPF provides virtually zero optimality gap (same values for Substation Power Cost, the objective function). Interestingly, the values of the control variable themselves, prominently, there is a significant difference in the suggested optimal reactive power control values for inverters associated with DERs and Batteries (results aggregated over all components over the horizon for conciseness). This highlights the fact that for a nonconvex nonlinear optimization problem may not necessarily have a unique global optimal point.

TABLE I: Comparative analyses between MPCOPF and MPDOPF - 5 time-period horizon

Metric	MPCOPF	MPDOPF
Biggest subproblem		
Decision variables	3150	1320
Linear constraints	5831	2451
Nonlinear constraints	635	265
Simulation results		
Substation power cost (\$)	576.31	576.30
Substation real power (kW)	4308.28	4308.14
Line loss (kW)	75.99	76.12
Substation reactive power (kVAR)	574.18	656.24
PV reactive power (kVAR)	116.92	160.64
Battery reactive power (kVAR)	202.73	76.01
Computation		
Number of Iterations	-	5
Total Simulation Time (s)	521.25	49.87

Table II showcases the feasibility of the control values suggested by the MPDOPF algorithm. First section 'Full horizon' describes the respective output variables for the entire horizon

from MPDOPF and OpenDSS. Second section 'Max. all-time discrepancy' stores the highest discrepancy between key state/output variables for all components across at any time-period between MPDOPF and OpenDSS. In both sections, the discrepancies are small enough to warrant feasibility of the obtained solution.

TABLE II: ACOPF feasibility analyses - 5 time-period horizon

Metric	MPDOPF	OpenDSS
Full horizon		
Substation real power (kW)	4308.14	4308.35
Line loss (kW)	76.12	76.09
Substation reactive power (kVAR)	656.24	652.49
Max. all-time discrepancy		
Voltage (pu)	0.0002	
Line loss (kW)	0.0139	
Substation power (kW)	0.3431	

To ensure that the complementarity of charging and discharging of batteries are being respected despite not using integer constraints, the charging/discharging profiles for batteries were checked, and indeed that is the case. Figure 1 is shown as one example.

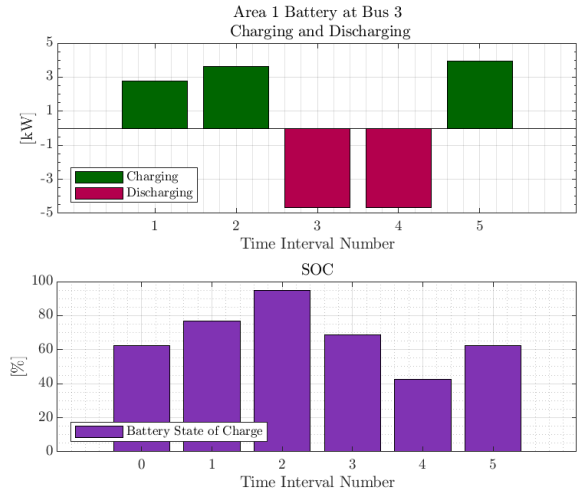


Fig. 1: Charging-Discharging and SOC graphs for Battery at Bus 3 located in Area 1 obtained by MPDOPF

The workflow of the MPDOPF algorithm, which involves exchange of boundary variables between parent-child area pairs, can be seen in the convergence plots in Figure 2.

Similarly, the convergence of the objective function to its optimal value with every iteration is shown by Figure 3.

B. Scalability Analysis

To demonstrate the effectiveness of the proposed algorithm over a bigger horizon to demonstrate scalability, simulations were run for a 10 time-period horizon. Figure 4 shows the forecasted profiles for load, solar irradiance and cost of substation power over the horizon.

From the comparison against MPCOPF in Table III, it can again be seen that MPDOPF is able to converge to the same

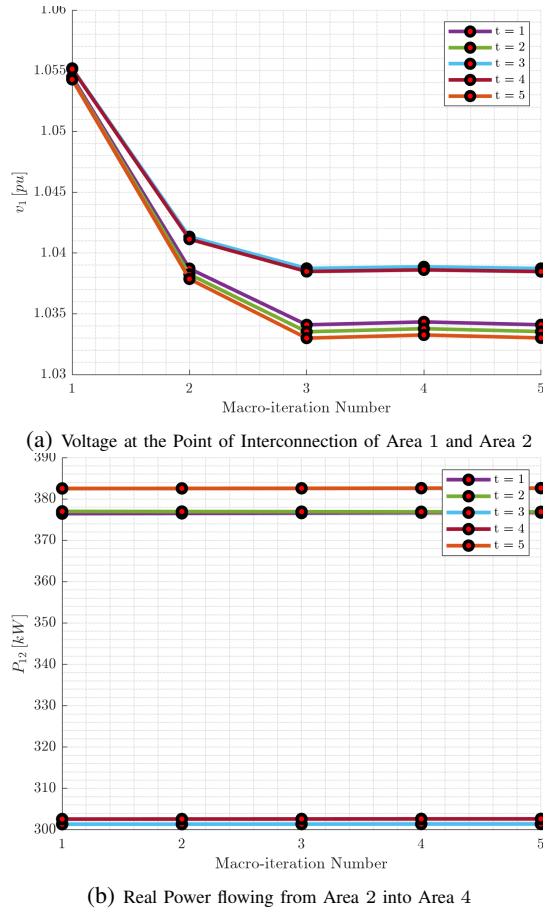


Fig. 2: Convergence of Boundary variables with every iteration. Each plot represents a particular variable exchanged between a pair of connected areas. Each line graph within a plot represents a particular time period.

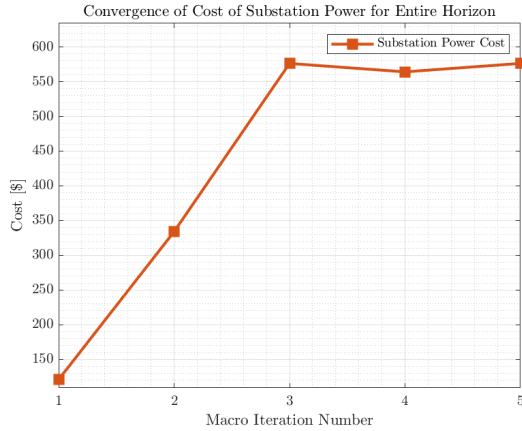


Fig. 3: Convergence of Objective Function Value with each MPDOPF iteration

optimal solution as MPCOPF. The computational speed up is even more pronounced than for the 5 time-period simulation.

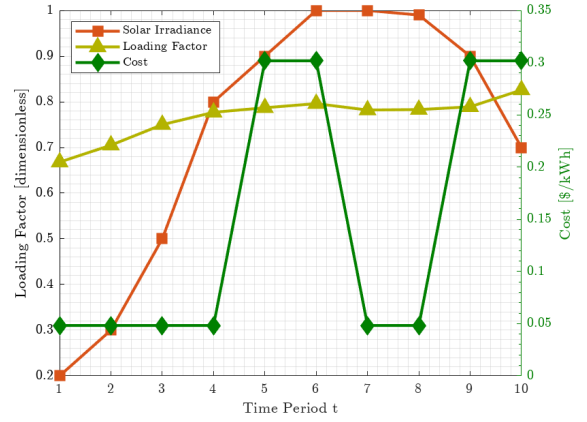


Fig. 4: Forecasts for Demand Power, Irradiance and Cost of Substation Power over a 10 Hour Horizon

TABLE III: Comparative analyses between MPCOPF and MPDOPF - 10 time-period horizon

Metric	MPCOPF	MPDOPF
Biggest subproblem		
Decision variables	6300	2640
Linear constraints	11636	4891
Nonlinear constraints	1270	530
Simulation results		
Substation power cost (\$)	1197.87	1197.87
Substation real power (kW)	8544.28	8544.04
Line loss (kW)	148.67	148.94
Substation reactive power (kVAR)	1092.39	1252.03
PV reactive power (kVAR)	222.59	139.81
Battery reactive power (kVAR)	388.52	310.94
Computation		
Number of Iterations	-	5
Total Simulation Time (s)	4620.73	358.69

Again, comparison against OpenDSS has yielded small discrepancies, attesting to the feasibility of the solution.

TABLE IV: ACOPF feasibility analyses - 10 time-period horizon

Metric	MPDOPF	OpenDSS
Full horizon		
Substation real power (kW)	8544.04	8544.40
Line loss (kW)	148.94	148.87
Substation reactive power (kVAR)	1252.03	1243.36
Max. all-time discrepancy		
Voltage (pu)		0.0002
Line loss (kW)		0.0132
Substation power (kW)		0.4002